(EO)6R 1998 Langmuir

DATASET · OCTOBER 2012

READS
22

7 AUTHORS, INCLUDING:

David J Vanderah
Institute for Bioscience and Biotechnology R…
90 PUBLICATIONS **1,860** CITATIONS
SEE PROFILE

Thomas B Parr
University of Delaware
38 PUBLICATIONS **46** CITATIONS
SEE PROFILE

Curtis W Meuse
National Institute of Standards and Technolo…
64 PUBLICATIONS **1,310** CITATIONS
SEE PROFILE

Gintaras Valincius
Vilnius University
82 PUBLICATIONS **1,089** CITATIONS
SEE PROFILE

Synthesis and Characterization of Self-Assembled Monolayers of Alkylated 1-Thiahexa(ethylene oxide) Compounds on Gold

David J. Vanderah,*,† Curtis W. Meuse,*,† Vitalii Silin,‡ and Anne L. Plant†

Biotechnology Division, Chemical Science and Technology Laboratory, National Institute of Standards and Technology, Gaithersburg, Maryland 20899, and Georgetown University, Washington, D.C. 20057

Received June 2, 1998. In Final Form: July 28, 1998

Self-assembled monolayers (SAMs) of a series of novel linear thiols containing a 1-thiahexa(ethylene oxide) (THEO) moiety, i.e., $HS(CH_2CH_2O)_6R$, where $R = C_{10}H_{21}$, $C_{10}D_{21}$, $C_{18}H_{37}$, and $C_{18}D_{37}$, were prepared on polycrystalline gold (Au) and characterized by reflection absorption infrared spectroscopy (RAIRS), spectroscopic ellipsometry, surface plasmon resonance (SPR), and contact angle measurements. The SAMs are hydrophobic with contact angles, θ_a (H_2O), of 108°−109° for all surfaces. For all compounds, our data provide evidence for well-ordered monolayers in which the THEO moiety is arranged in a 7/2 helix oriented normal to the substrate. The alkyl group conformation and tilt are similar to the corresponding *n*-alkanethiol SAMs.

Introduction

The study of supported phospholipid/organic thiol hybrid bilayer membranes (HBMs) has intensified over the past few years. These model systems are being used for the study of membrane proteins and the development of sensors, bioelectronics, and bioprocessing devices based on cell membrane components.[1−23] HBMs are attractive for both fundamental studies and applications because (1) they are reasonable models of natural bilayers, (2) their composition and physical characteristics can be designed and controlled, (3) they are stabilized by the strong interaction of the alkanethiol with the metal support, and (4) they are amenable to study by a wide variety of surface science techniques. HBM construction utilizes the well-characterized self-assembly[24−27] of organic thiols and disulfides on metal surfaces to produce a hydrophobic surface for the assembly of a second layer of phospholipid. We have studied HBMs by a number of techniques, including electrochemistry,[16−18] surface plasmon resonance (SPR),[19] reflection absorption infrared spectroscopy (RAIRS),[20,21] surface enhanced Raman spectroscopy (SERS),[20] spectroscopic ellipsometry,[21] and neutron reflectivity.[21] The electrochemical insulating characteristics of our HBMs are consistent with those of other model lipid bilayer membranes and are affected by divalent cations[17] and the peptide toxin melittin.[18] Transmembrane protein activity has been observed in HBMs prepared with alkanethiol self-assembled monolayers (SAMs).[22,23] However, the lipids of biological membranes are in the fluid phase, in contrast to the alkanethiol monolayer HBMs, which are highly ordered. HBMs containing less ordered SAMs may improve the efficiency of protein incorporation. In addition, transmembrane proteins span the membrane and contact an aqueous environment on both sides of natural lipid bilayers. Providing an aqueous layer on the proximal side of a supported HBM may improve the efficiency of incorporated protein activity. SAMs composed of compounds with a

* To whom correspondence should be addressed.
† National Institute of Standards and Technology.
‡ Georgetown University

(1) Raguse, B.; Braach-Maksvytis, V.; Cornell, B. A.; King, L. G.; Osman, P. D. J.; Pace, R. J.; Wieczorek, L. *Langmuir* **1998**, *14*, 648.
(2) Cornell, B. A.; Braach-Maksvytis, V. L. B.; King, L. G.; Osman, P. D. J.; Ragues, B.; Pace, R. J. *Nature* **1997**, *387*, 580.
(3) Bunjes, N.; Schmidt, E. K.; Jonczyk, A.; Rippmann, F.; Ringsdorf, H.; Grauber, Knoll, W.; Naumann, R. *Langmuir* **1997**, *13*, 6188.
(4) Cheng, Y.; Boden, N.; Bushby, R. J.; Clarkson, S.; Evans, S. D.; Knowles, P. F.; Marsh, A.; Miles, R. E. *Langmuir* **1998**, *14*, 839.
(5) Williams, L. M.; Evans, S. D.; Flynn, T. M.; Marsh, A.; Knowles, P. F.; Bushby, R. J.; Boden, N. *Langmuir* **1997**, *13*, 751 and all references therein.
(6) Lang, H.; Duschle, C.; Gratzel, M.; Vogel H. *Thin Solid Films* **1992**, *210/211*, 818.
(7) Spinke, J.; Yang, J.; Wolf, H.; Liley, M.; Ringsdorf, H.; Knoll, W. *Biophys. J.* **1992** *63*, 1667.
(8) Florin, E.-l.; Gaub, H. E. *Biophys. J.* **1993**, *64*, 375.
(9) Stelzle, M.; Weissmuller, G.; Sackmann, E. *J. Phys. Chem.* **1993**, *97*, 2974.
(10) Lang, H.; Duschl, C.; Vogel, H. *Langmuir* **1994**, *10*, 197.
(11) Erdelen, C.; Haussling, L.; Naumann, R.; Ringsdorf, H.; Wolf, H.; Yang, J.; Liley, M.; Spinke, J.; Knoll, W. *Langmuir* **1994**, *10*, 1246.
(12) Duschl, C.; Liley, M.; Corradin, G.; Vogel, H. *Biophys. J.* **1994**, *67*, 1229.
(13) Naumann, R.; Jonczyk, A.; Kopp, R.; van Esch, J.; Ringsdorf, H.; Knoll, W.; Graber, P. *Angew. Chem. Int. Ed. Eng.* **1995**, *34*, 2056.
(14) Duschl, C.; Liley, M.; Lang, H.; Ghandi, A.; Zakeeruddin, S. M.; Stahlberg, H.; Dubochet, J.; Nemetz, A.; Knoll, W.; Vogel, H. *Mater. Sci. Eng.* **1996**, *C*4, 7.
(15) Rothe, U.; Aurich, H. *Biotechnol. Appl. Biochem.* **1989**, *11*, 18.
(16) Plant, A. L. *Langmuir* **1993**, *9*, 2764.
(17) Plant, A. L.; Gueguetchkeri, M. *Proceedings of the Thirteenth Southern Biomedical Engineering*, 1994, University of the District of Columbia, Washington, DC.
(18) Plant, A. L.; Gueguetchkeri, M.; Yap, W. *Biophys. J.* **1994**, *67*, 1126.
(19) Plant, A. L.; Brigham-Burke, M.; O'Shannessy D. *Anal. Biochem.* **1995**, *226*, 342.
(20) Meuse, C. W.; Niaura, G.; Lewis; M. L., Plant, A. L. *Langmuir* **1998**, *14*, 1604.
(21) Meuse, C. W.; Krueger, S.; Majkrzak, C. F.; Dura, J.; Fu, J.; Conner, J. T.; Plant, A. L. *Biophys. J.* **1998**, *74*, 1388.
(22) Rao, N. M.; Plant, A. L.; Silin, V.; Wight, S.; Hui, S. W. *Biophys. J.* **1997**, *73*, 3066.
(23) Kinnear, K. T.; Monbouquette, H. G. *Anal. Chem.* **1997**, *69*, 1771.
(24) Nuzzo, R. G.; Fusco, F. A.; Allara, D. L. *J. Am. Chem. Soc.* **1987**, *109*, 2358.
(25) Porter, M. D.; Bright, T. B.; Allara, D. L.; Chidsey, C. E. D. *J. Am. Chem. Soc.* **1987**, *109*, 3559.
(26) Bain, C. D.; Troughton, E. B.; Tao, Y.-T.; Evall, J.; Whitesides, G. M.; Nuzzo, R. G. *J. Am. Chem. Soc.* **1989**, *111*, 321.
(27) Collins, R. W.; Allara, D. L.; Kim, Y.-K.; Lu, Y.; Shi, J. *Characterization of Organic Thin Films*; Ulman, A., Ed.; Butterworth-Heineman: Boston, 1995; pp 48, 49.
(28) Kunitake, T. *Angew. Chem., Int. Ed. Engl.* **1992**, *31*, 709.

10.1021/la9806451 CCC: $15.00
Published on Web 11/24/1998

hydrophilic region or "spacer" close to the substrate (Au) would be expected to be more fluid than alkanethiols (vide infra) as well as providing a more hospitable environment for the incorporation of water and extramembranous protein segments on the proximal side of the HBM. Different approaches to providing a hydrophilic spacer near the Au have been described.[1−5,10,12−15]

Structural motifs incorporating ionic and nonionic functionalities, in various structural strategies, which result in bilayer-forming compounds are richly illustrated in a recent review.[28] All polar functionalities are a departure from the *n*-alkyl framework, to a greater or lesser extent, and thus might be expected to result in a decrease in the order and/or packing of the alkane chains. While a decrease in the packing order is desirable, perhaps even necessary, for integral membrane protein incorporation into the HBM (vide supra), the degree of disorder in the SAM will have some lower limit, i.e., it could be disordered to the extent that protein−substrate interactions are insufficiently screened.[14] The fundamental objective in amphiphile design for HBMs is functionality selection that will substantially increase hydrophilicity while more subtly decreasing the order of the SAM. However, there are no correlations between functional groups and SAM order to guide this selection and one may not be able predict the extent of disorder on the basis of the molecular structure. Even the length of the spacer required is not obvious.

SAMs and mixed SAMs of thiols containing oligo(ethylene oxides) (OEOs) as hydrophilic spacers or "anchor segments" have been reported.[1−5,10,14,29,30] Most of these[1−5,10,14] are directed toward supported bilayer constructs. The thiolipids {$[R(EO)_xS]_2$, where R = dialkylglycerophosphatidyl, EO = $-OCH_2CH_2-$ and x = 1, 2, or 3} and the SAMs and lipid bilayers derived therefrom are the most well characterized.[10,14] Other approaches have utilized spacers consisting of OEO segments of three and four EO units connected by C_4 diester linkages[1,2] or 1-thia-OEO derivatives of cholesterol.[4,5] For all these studies, the spacers contained at least one hydrophilic non-EO functional group.

In this study, we synthesized a series of thiol compounds having the structure $HS(CH_2CH_2O)_xR$, where R = *n*-alkyl group and x = 6. This hydrophilic spacer, 1-thiahexa(ethylene oxide) (THEO), retains a linear framework, i.e., *n*-alkane-like with all atoms other than hydrogen in a linear arrangement, and is expected to provide good monolayer coverage. On the basis of previous work,[31,32] we anticipated that the SAMs of compounds containing this spacer would most likely be less ordered and more "flexible"[32] than *n*-alkanethiols as the result of an increased population of gauche configurations around the ether oxygens in the THEO segment. Also there is a reasonable possibility that one may be able to intentionally vary the order of the spacer by the addition water,[14] buffer, and/or cations (Li^+, Na^+, or K^+).[33] In addition, since this hydrophilic spacer is composed only of EO units, this study allows us to directly access the structure of this motif.

As part of an effort to construct HBMs containing a hydrophilic region near the Au substrate, we herein describe the synthesis of this new class of thiol compound,

Scheme 1[a]

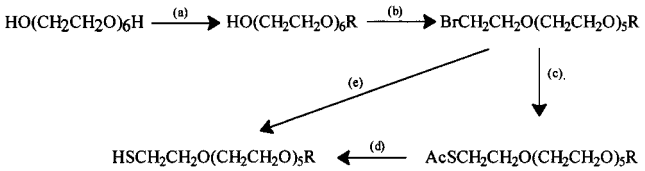

[a] Reagents: (a) 50% aq NaOH, 100−105 °C, 0.5 h, cool then add RBr, where R = $C_{10}H_{21}$, $C_{10}D_{21}$, $C_{18}H_{37}$, or $C_{18}D_{37}$ and [NaOH]/[RBr] = 1/1, 100−105 °C, 24−36 h (50−65%); (b) 1.3 mol trifluoroacetic anhydride/THF, rt, 1−2 h, followed by 5 mol LiBr/THF−HMPA, reflux, 1−12 h (85−90%); (c) 1.2 mol NaSAc/MeOH, reflux, 1 h (>95%); 0.1 M HCl/MeOH, rt, 3−5 d (>90%); (e) 2.1 mol NaSAc/MeOH, reflux, 4−16 h (80−95%).

where R = $C_{10}H_{21}$ (**1**), $C_{10}D_{21}$(**2**), $C_{18}H_{37}$ (**3**), and $C_{18}D_{37}$ (**4**), and report the structural characteristics of the SAMs of **1**−**4** on polycrystalline Au as deduced from RAIRS, SPR, spectroscopic ellipsometry, and contact angle data.

Materials and Methods[34]

Hexa(ethylene oxide), 1-bromodecane, 1-bromooctadecane, thiolacetic acid (Aldrich Chemical Co., Milwaukee, WI), 1-bromodecane-d_{21}, and *n*-octadecanol-d_{37} (Cambridge Isotope Laboratories, Cambridge, MA) were purchased and used as received. 1-Bromooctadecane-d_{37} was prepared from *n*-octadecanol-d_{37} by established procedures.[35] Tetrahydrofuran (THF) (Mallinckrodt AR) and hexamethylphosphoramide (HMPA) (Aldrich) were dried by distillation from sodium hydride. The THF was distilled immediately before use, the HMPA was distilled and stored under nitrogen over 3 Å molecular sieves. All other solvents (AR grade) were used without purification.

Synthesis. Compounds **1**−**4** (alkylated 3,6,9,12,15,18-hexaoxaoctadecane-1-thiols) were prepared in four or five steps as outlined in Scheme 1. All yields are good to excellent and are easily carried out on a moderate scale. Alkylation of hexa(ethylene oxide) and subsequent conversion to a bromo compound were carried out according to published procedures.[31,35] Preparation of the thiol from the bromo compound was effected either by conversion to the thiol acetate ($NaSCOCH_3$/MeOH) followed by mild acidic methanolysis as previously described[31] or by a new two-step, one-pot procedure (2 mol of $NaSCOCH_3$/MeOH) recently developed in our laboratory.[36] The preparation of **3** is illustrative of the latter. To 50 mL of methanol was added 0.2342 g (0.102 mol) of Na^0. After the evolution of H_2 had ceased, 0.756 g (0.0099 mol) of thiolacetic acid was added via syringe. To this slightly yellow solution was added a solution of 2.57 g (0.0043 mol) of $BrCH_2CH_2O(CH_2CH_2O)_5C_{18}H_{37}$ in 10 mL of methanol. The reaction mixture was degassed and flushed with argon (Ar) (three times) then refluxed for 7 h. After cooling to room temperature, the reaction mixture was poured into a cold mixture of ether (50 mL) and water (50 mL) containing 1 mL of concentrated HCl. The product **3** [2.237 g 94%; >95% pure, thin-layer chromatography (TLC) analysis], was obtained by standard extractive techniques. Additional examples as well as the scope and limitations of this methodology will be published elsewhere.

All compounds were purified by chromatography (silica gel) and structural assignments were made from nuclear magnetic resonance (NMR), infrared (IR), and mass spectroscopy analysis. The NMR and mass spectroscopy data for **1**−**4** are shown in

(29) Lu, T.; Zhang, L.; Gokel, G. W.; Kaifer, A. E. *J. Am. Chem. Soc.* **1993**, *115*, 2542.

(30) Zhang, L.; Lu, T.; Gokel, G. W.; Kaifer, A. E. *Langmuir* **1993**, *9*, 786.

(31) Pale-Grosdemange, C.; Simon, E. S.; Prime, K. L.; Whitesides, G. M. *J. Am. Chem. Soc.* **1991**, *113*, 12 and references therein.

(32) Laibinis, P.; Bain, C. D.; Nuzzo, R. G.; Whitesides, G. M. *J. Phys. Chem.* **1995**, *99*, 7663.

(33) All fast atom bombardment (FAB) mass spectra of compounds containing the hexa(ethylene oxide) [HEO] moiety or the THEO moiety, give only an $M^+ + Na^+$ peak. The complete absence of a molecular ion suggests strong affinity for complexation to Na^+ and perhaps other alkali earth cations. The HEO/THEO moiety is similar to crown ethers which are known to tightly complex alkali earth cations; such complexation on exposure to buffers or solutions containing Na^+ could lead to significant changes in the three-dimensional structure of the OEO segment.

(34) The specification of commercial products is for clarity only and does not constitute endorsement by NIST.

(35) Camps, F.; Gasol, V.; Guerrero, A. *Synthesis* **1987**, 511.

(36) Vanderah, D. J.; Afeefy, H. presented at the 29th Middle Atantic Regional Meeting American Chemical Society Meeting, American University, May 22, 1995, unpublished.

Table 1. NMR ($CDCl_3$) and Mass Spectrometry Data for 1−4

1 δ 3.66−3.56. (22H, m, $HSCH_2C\mathbf{H}_2O(C\mathbf{H}_2C\mathbf{H}_2O)_5C_{10}H_{21}$), 3.44 (2H, t, J = 6.8 Hz, $HS(CH_2CH_2O)_6C\mathbf{H}_2CH_2(CH_2)_7CH_3$), 2.70 (2H, dt, J = 8.2 & 6.4 Hz, $HSC\mathbf{H}_2CH_2O(CH_2CH_2O)_5C_{10}H_{21}$), 1.60 (1H, t, J = 8.2 Hz, $\mathbf{H}SCH_2CH_2O(CH_2CH_2)_5C_{10}H_{21}$), 1.58 (2H, m, $HS(CH_2CH_2O)_6CH_2C\mathbf{H}_2(CH_2)_7CH_3$), 1.26 (14H, br s, $HS(CH_2CH_2O)_6CH_2CH_2(C\mathbf{H}_2)_7CH_3$); 0.88 (3H, t, J = 6.7 Hz, $HS(CH_2CH_2O)_6CH_2CH_2(CH_2)_7C\mathbf{H}_3$); HR CI [M + H$^+$] calcd for $C_{22}H_{47}O_6S$ 439.30933. Found 439.30838.

2 δ 3.66−3.56. (22H, m, $HSCH_2C\mathbf{H}_2O(C\mathbf{H}_2C\mathbf{H}_2O)_5C_{10}D_{21}$), 2.70 (2H, dt, J = 8.1 & 6.3 Hz, $HSC\mathbf{H}_2CH_2O(CH_2CH_2O)_5C_{10}D_{21}$), 1.60 (1H, t, J = 8.2 Hz, $\mathbf{H}SCH_2CH_2O)_5C_{10}D_{21}$); HR CI [M + H$^+$] calcd for $C_{22}H_{26}O_6SD_{21}$ 460.44116. Found 460.43997.

3 δ 3.64−3.54 (22H, m, $HSCH_2C\mathbf{H}_2O(C\mathbf{H}_2C\mathbf{H}_2O)_5C_{18}H_{37}$), 3.41 (2H, t, J = 6.7 Hz, $HS(CH_2CH_2O)_6C\mathbf{H}_2CH_2(CH_2)_{15}CH_3$), 2.68 (2H, dt, J = 8.2 & 6.5 Hz, $HSC\mathbf{H}_2CH_2O(CH_2CH_2O)_5C_{18}H_{37}$), 1.56 (1H, t, J = 8.2 Hz, $\mathbf{H}SCH_2CH_2O)_6C_{18}H_{37}$), 1.58 (2H, m, $HS(CH_2CH_2O)_6CH_2C\mathbf{H}_2(CH_2)_{15}CH_3$), 1.22 (30H, br. s, $HS(CH_2CH_2O)_6CH_2CH_2(C\mathbf{H}_2)_{15}CH_3$); 0.85 (3H, t, J = 6.7 Hz, $HS(CH_2CH_2O)_6CH_2CH_2(CH_2)_{15}C\mathbf{H}_3$); HR CI [M + H$^+$] calcd for $C_{30}H_{63}O_6S$ 551.43451. Found 551.43428.

4 δ 3.65−3.58 (22H, m, $HSCH_2C\mathbf{H}_2O(C\mathbf{H}_2C\mathbf{H}_2O)_5C_{18}D_{37}$), 2.69 (2H, dt, J = 8.1 & 6.5 Hz, $HSC\mathbf{H}_2CH_2O(CH_2CH_2)_5C_{18}D_{37}$), 1.59 (1H, t, J = 8.2 Hz, $\mathbf{H}SCH_2CH_2O)_6C_{18}D_{37}$); HR EI [M$^+$] calcd for $C_{30}H_{25}O_6SD_{37}$ 587.65894. Found 587.65961.

Table 1. The related compound $HS(CH_2)_{11}(OCH_2CH_2)_6OH$, **5**, was prepared as described by Pale-Grosdemange et al.[31]

Molecular Modeling. The THEO segment of the SAMs of **1**−**4** were modeled using Hyperchem (Hypercube, Gainesville, FL).

Sample Preparation. Gold substrates were used in all measurements. For the SPR measurements, ∼450 Å of gold (99.99%) was deposited by magnetron sputtering (Edwards Auto 306) at a base pressure of 3.6×10^{-3} mbar Ar^+ on polished glass (20 mm × 14 mm × 2 mm) that was cleaned with glow discharge plasma. The film growth rate was ∼100 Å/s, which was followed by an annealing time (45 min). Reproducible results were obtained when the freshly deposited gold-on-glass samples were immersed in absolute ethanol immediately after removal from the vacuum chamber. Prior to use, the substrates were removed from the ethanol, dried in a stream of dry nitrogen, and promptly introduced into the SPR device equipped with a flow cell (0.036 mL) as described previously.[37] For all other measurements, gold substrates were prepared on silicon (1 0 0) wafers (Virginia Semiconductor, Fredricksburg, VA) previously coated with a layer of chromium either by magnetron sputtering or by thermal evaporation at a base pressure of $\sim 1.3 \times 10^{-6}$ mbar to a nominal thickness of 2000 Å. For the contact angle measurements and the RAIRS experiments monolayers were prepared by immersing the gold substrates in $\sim 1 \times 10^{-3}$ mol/L (mM) thiol solutions in 200 proof ethanol (Warner Graham Co., Cockeysville, MD) for a minimum of 12 h. For the ellipsometry measurements 1 mM or 1 μM thiol solutions in ethanol were used. For the latter, the Au substrates were immersed for a minimum of 7 days.

Contact Angle Measurements. Contact angles were determined with a Ramé-Hart model 110-00-115 goniometer at room temperature and ambient relative humidity using water as the probing liquid. Advancing contact angles (θ_a) were measured by lowering a 2−3 μL drop onto the surface from a blunt-ended needle attached to a 2 mL syringe. The contact angle was recorded immediately after the drop detached from the needle tip. At least four measurements were taken for each SAM; the value of θ_a was the average of these measurements.

Spectroscopic Ellipsometry. Multiple wavelength ellipsometric measurements were performed on a J. A. Woollam Co., Inc. (Lincoln, NE) M-44 spectroscopic ellipsometer aligned at an incidence angle 70.390° from the surface normal. Thicknesses were calculated relative to a 1-propanethiol SAM on Au using a two-layer model in which the optical constants of the Au layer were determined using a refractive index of 1.45 and a thickness of 6 Å for the propanethiol SAM. The optical constants for the Au were then used to determine the thickness of the SAM, assuming a refractive index of 1.45 for all alkanethiols and **1**−**5**. Using this protocol, the ellipsometric thickness of dodecanethiol was found to be 17 ± 2 Å, as has been previously reported.[27] Modeling and thickness calculations were done using the WVASE software from J. A. Woollam Co.

RAIRS Measurements. The FTIR spectra were obtained on a Bruker Equinox 55 spectrometer (Billerica, MA) with a home-built external reflection accessory consisting of a wire grid polarizer (Pike Scientific, Madison, WI), a slit, and an optical labjack. The polarizer was placed before the sample and set to select infrared radiation polarized parallel to the plane of incidence. The slit, ∼1.5 mm high and 8 mm wide, was positioned on the front edge of the labjack with its long bottom edge parallel to its surface. The labjack was positioned in the sampling compartment so that the center of the sample was at the focus of the instrument. When the samples were placed on the surface of the labjack, the height of the jack was adjusted until the focus of the instrument provided near-glancing angle illumination of the sample and the slit prevented overfilling of the sample. Spectra were obtained using 755 sample and 755 background scans (10 min collection time) at 2 cm^{-1} resolution. All spectral analysis was performed using Grams 386 software (Galactic Industries, Salem, NH). Spectral simulations were performed using a method developed by Parikh and Allara implemented in MathCad (MathSoft, Cambridge, MA) in our laboratory.[25,38]

Surface Plasmon Resonance. The SPR device and the calibration of the SPR shift with respect to the optical thickness change were described previously.[37] Data collection [acquisition rate ∼1/s and charge-coupled device (CCD) acquisition time of 1×10^{-3} s] was initiated with the establishment of a baseline with an initial flow of anhydrous ethanol over the bare gold surface (flow rate = 2.4 μL/s for 20 min). Flow was then switched to an alkanethiol solution (∼1 mM in ethanol). Subsequent operations included washing with anhydrous ethanol, and for some samples, flow and data collection were stopped and then continued after 14 h. Film thickness calculations were carried out assuming a refractive index of 1.45 for the organic film.

Results and Discussion

We will largely restrict our discussion in this section to **1** and **3** since, except for the expected IR and NMR spectral differences, the results were similar between these compounds and their deuterated counterparts **2** and **4**, respectively. The monolayer thicknesses and the kinetics of SAM formation were studied with the surface plasmon resonance (SPR) technique in real time under continuous flow. Thicknesses[39] for **1**, **3**, octadecanethiol, and $HS(CH_2)_{11}(OCH_2CH_2)_6OH$ (**5**) as a function of time are shown in Figure 1. All compounds show a kinetic profile consistent with previous observations for thiol-on-Au SAMs.[27,40] These data show that the kinetics of formation for each compound is different and all indicate nonzero slopes after 25 min, suggesting physisorption and the formation of more than a monolayer.[41]

The rates of thickness increase in the following order **3** ≈ C_{18} > **5** > **1** and are generally consistent with the relative solubilities of the alkanethiols in ethanol (**1** ≥ **5** > **3** ≥ C_{18}) as has been previously observed.[40] Figure 2 shows thickness increases for **1** and **5**. The difference in the rates for **1** and **5** is interesting since these two compounds would be expected to have essentially the same solubility in ethanol. A possible rationale for the slower kinetics of **1** relative to **5** (from ethanol) may be due to

(37) Silin, V.; Weetall, H.; Vanderah, D. J. *J. Colloid Interface Sci.* **1997**, *185*, 94.

(38) Parikh, A. N.; Allara, D. L. *J. Chem. Phys.* **1992**, *96*, 927.

(39) While we will use the term thickness throughout, the term effective thickness would be more precise. The effective thicknesses of our films are calculated from the change in the angle of reflectivity, $\Delta\theta$, which is measured directly in the SPR experiment.

(40) Peterlinz, K. A.; Geordiadis, R. *Langmuir* **1996**, *12*, 4731.

(41) Our data indicate little or no physisorption for octadecanethiol; however, physisorption for octadecanethiol has been reported.[40] This probably reflects differences in observation times (50 min vs 72 h[40]).

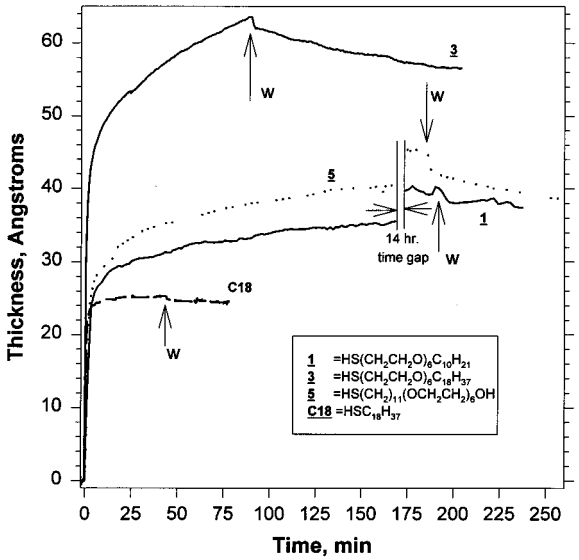

Figure 1. SPR surface thickness measurements of $C_{10}H_{21}(OCH_2CH_2)_6SH$ (**1**), $C_{18}H_{37}(OCH_2CH_2)_6SH$ (**3**), $HO(CH_2CH_2O)_6(CH_2)_{11}SH$ (**5**), and $C_{18}H_{37}SH$ under continuous flow conditions as a function of time. Thickness was calculated from the position of the SPR minimum and an assumed refractive index of 1.45 for the SAM. The initiation of flow of a 1 mM alkanethiol solution defines $t = 0$. W = washing with anhydrous ethanol. || = 14 h period of no flow.

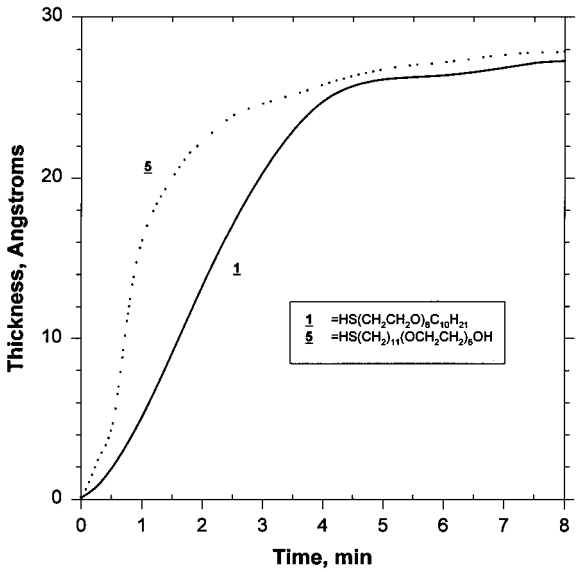

Figure 2. SPR surface thickness measurements of $C_{10}H_{21}(OCH_2CH_2)_6SH$ (**1**) and $HO(CH_2CH_2O)_6(CH_2)_{11}SH$ (**5**) under continuous flow conditions as a function of time from 0 to 8 min. Thickness was calculated from the position of the SPR minimum and an assumed refractive index of 1.45 for the SAM. The initiation of flow of a 1 mM alkanethiol solution defines $t = 0$.

differences in the solvation of the thiol groups. The thiol group in **1** is located in a region of the molecule that would be more highly (or more strongly) solvated than the thiol group in **5**. More extensive or more tightly held solvation shells at or near the thiol group would impede the chemisorption process.

From the SPR data, monolayer thickness and desorption kinetic constants were calculated for **1**, **3**, and **5** using a single exponential model for kinetic desorption of physisorbed molecules on top of irreversibly chemisorbed molecules. The thickness values are shown in Table 2; the desorption kinetic constants were found to be 1.1 ± 0.5×10^{-4}/s for all compounds. The presence of physisorbed molecules is denoted by the fact that the observed thicknesses for **1**, **3**, and **5** exceed theoretical limits (for the latter see Table 2). Physisorption is most pronounced for **3** and, for all compounds, is removed only slowly by washing with ethanol.

Table 2. Wetting and Monolayer Thickness for 1−5 and Selected Alkyl Thiols

	H_2O contact angles[a] (advancing, deg)	*d* (Å)		
		Th[b]	El[c]	SPR[d]
1	108	36	31	31 ± 5
2	108	36	31	
$C_{12}H_{25}SH$	108	–	17	
3	109	46	41	50 ± 2
4	108	46	42	
$C_{18}H_{37}SH$	113	–	23	
5	22[e,f]	39	27[31]	32 ± 1

[a] Values are ±2°. [b] Th = theoretical. Maximum monolayer thicknesses were calculated using Hyperchem with each molecule constrained to (1) a fully extended all-trans-conformation and (2) oriented normal to the substrate. [c] El = ellipsometry. Values are ±2 Å. [d] SPR = surface plasmon resonance. [e] Reported 34−38°.[31] [f] Error in this measurement >2°.

Film thicknesses of **1**−**4** and octadecanethiol, as calculated from ellipsometric data, are also shown in Table 2. The thicknesses of **1** and **3** were found to be 31 and 41 ± 2 Å, respectively. During the course of our ellipsometric data collection, we observed that when the Au surface was in contact with the alkanethiol solution for extended periods (> 48 h), measurements gave thickness values larger than those reported in Table 2, particularly for the longer alkyl chain compounds **3** and **4**. These values changed only slowly with simple washing, as has been observed previously,[24] but were found to return to the values in Table 2 with sonication (2 min to 15 min) in ethanol. This supports our SPR observations indicating gradual development of more than monolayer coverage.

Film thicknesses from the ellipsometric data and SPR data are in general agreement. The thickness of **1** was found to be the same for both ellipsometry and SPR whereas higher values for **3** and **5** were obtained from the SPR data.[42] The slightly higher value for **5** may reflect the influence of solvent. We would expect that **5** would have a stronger interaction with ethanol than **1** or **3** because it presents a hydrophilic surface to it. The more significant thickness difference for **3** is attributed to physisorption, as mentioned earlier.

Contact angle [θ_a, (H_2O)] data for the SAMs of **1**−**4**, dodecanethiol, and octadecanethiol are shown in Table 2. The large θ_a for all compounds indicate, as expected, that the SAMs present a hydrophobic surface to the probing liquid. The identical θ_a of 108° for **1**−**4** and dodecanethiol indicates that these SAMs have comparable surface energies. The presence of physisorbed molecules was also indicated from contact angle data. The θ_a of the SAMs decreased to 103°−105° when kept in contact with the hexaoxaalkanethiol solutions for extended periods of time,

(42) Comparison of film thicknesses by ellipsometry and SPR are subject to a number of constraints. First, the optical constants of the gold change during SAM formation. These changes are compensated for in the ellipsometry by the fact that the optical constants of the gold were calculated with an alkanethiol (1-propanethiol) adsorbed to it. Second, in the SPR experiment the film is in constant contact with solvent (and alkanethiol) during formation whereas for ellipsometry the SAM is washed and dried before data collection. We would expect that the thickness values from SPR data would be higher than from ellipsometry data, especially for SAMs with strong solvent interactions. This has recently been reported.[40] For **5**, our SPR thickness is slightly higher than the ellipsometric thickness reported earlier.[31]

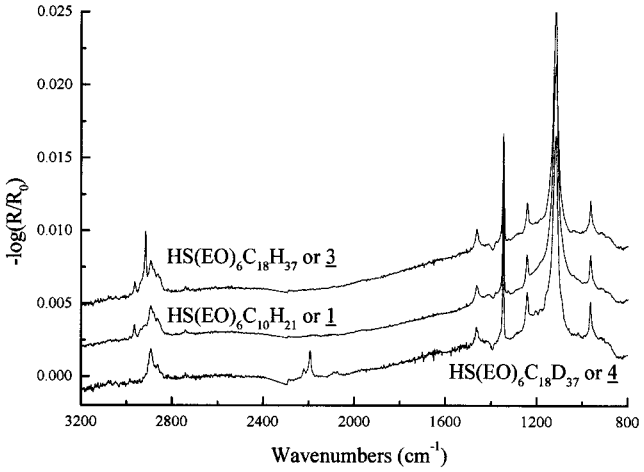

Figure 3. RAIRS spectra of $C_{10}H_{21}(OCH_2CH_2)_6SH$ (**1**), $C_{18}H_{37}(OCH_2CH_2)_6SH$ (**3**), and $C_{18}D_{37}(OCH_2CH_2)_6SH$ (**4**) SAMs from 3200 to 800 cm^{-1}.

but sonication of these SAMs returned the θ_a to those reported in Table 2 (data not shown).

The molecular structure of the SAMs was probed with infrared spectroscopy. The infrared reflectance spectra of **1**−**4** are similar. Figure 3 shows the RAIRS spectra of **1**, **3**, and **4** on Au. The spectra of **1** and **3** are essentially identical and only show differences in the C−H stretching region (3050−2750 cm^{-1}) due to the longer alkyl chain in **3**. Comparison of the spectra of **3** and **4** reveals the expected differences due to the presence of deuterium in **4**. In the spectrum of **4**, the absorption bands in the C−H stretching region (3050−2750 cm^{-1}) are now due solely to the C−H bonds in the THEO segment, and the new peaks appearing near 2200 cm^{-1} are the C−D stretching bands of the C_{18} alkyl chain. Peak frequencies along with suggested mode assignments for the isotopic and monolayer samples of **3** on Au are shown in Table 3.

The structure and orientation of the THEO segment is obtained from analysis of the 1600−800 cm^{-1} region. Interpretation of this region is derived from the crystal structure of poly(ethylene oxide) PEO,[43] and a recent IR study of different polymorphic forms of crystalline PEO.[44] X-ray diffraction of PEO crystals indicates a unit cell of four molecules having a 7/2 helical conformation, i.e., seven ethylene oxide units turn two times per fiber period.[43] PEO has various crystalline morphologies between two extreme cases, the extended-chain crystal (ECC) polymorphic form and the folded-chain crystal (FCC) polymorphic form, which differ markedly in the 1400−800 cm^{-1} region of their IR spectra. The IR bands corresponding to the E_1 symmetry species of the line group $D(4\pi/7)$[45] are the same for the two polymorphs. However, bands from the A_2 symmetry species appear at higher frequencies in the FCC form than the ECC form. The E symmetry bands have transition moments perpendicular to the chain axis while the transition moments of the A species bands are parallel to the chain axis. The difference in A band positions have been quantitatively rationalized as due to transition dipole−dipole coupling arising from the alignment of the helices relative to the long axis in the FCC−PEO.[44]

Table 3. Peak Assignments for 3 in KBr (Isotropic Sample) and on Au

frequency (cm^{-1})		
3 in KBr	**3** on Au	peak assignments[a]
2962 (sh)	2964	r^-_a, CH_3, C−H str (asym, ip)[b]
2954	∼2957 (sh)	r^-_b, CH_3, C−H str (asym, op)[b]
2934	2938	r^+_{FR}, CH_3, C−H str (sym FR)[b]
2916	2917	d^-, CH_2, C−H str (asym)[b]
2892		d^+_{FR}, CH_2, C−H str (sym FR)[b]
	2878	r^+_{FR}, CH_3, C−H str (sym FR)[b]
2850	2851	d^+, CH_2, C−H str (sym)[b]
2803		
2741		
2721		
2696		A_2 (4) overtone[c]
2636		
2557		H−S str[d]
1472		CH_2 bending[b]
1466		CH_2 scissors def, δ_{CH_3}[b]
1458	1460	
1419		C−S asym def or α-CH_2 scissoring
1358		$E_1(8)$[c]
1347	1345	$A_2(4)$[c]
1302		CH_2 twisting-rocking
1292		
1280		$E_1(9)$[c]
1242	1243	$A_2(5)$[c]
1237		$E_1(10)$[c]
1147		$E_1(11)$[c]
1116[e]	1118	$A_2(6)$[c]
1066		$E_1(13)$[c]
965	966	$A_2(7)$[c]
952		
946 (sh)		$E_1(14)$[c]
852		
843		$E_1(15)$[c]
717		CH_2 rocking−twisting

[a] Mode assignment nomenclature: str = stretch, sh = shoulder, asym = antisymmetric, sym = symmetric, FR = Fermi resonance, def = deformation. [b] References 25 and 46. [c] Reference 44. [d] Silverstein, R. M.; Bassler, G. C.; Morrill, T. C. *Spectrometric Identification of Organic Compounds*, 4th ed.; Wiley & Sons: New York, 1981; p 131. [e] $A_2(6) + E_1(12)$.

The isotropic spectrum of **3** (Table 3) shows all the A_2 and E_1 absorption bands in PEO. The presence of peaks at 1347, 1242, and 965 cm^{-1}—assigned to the $A_2(4)$, $A_2(5)$, and $A_2(7)$ absorption bands, respectively—as well as the presence of the $A_2(6)$ band at 1116 cm^{-1} indicate that **3** exists, in the solid state, in the FCC polymorphic form. The FCC polymorphic form is also indicated in the spectra of **1**, **3**, and **4** on Au (Figure 4). The position of the absorption bands for $A_2(4)$, $A_2(5)$, $A_2(6)$, and $A_2(7)$ nearly perfectly match those of FCC−PEO.[44] This indicates that the structure of the THEO segment of the SAM is identical with FCC−PEO, i.e., with EO units aligned such that corresponding oxygens from molecule to molecule are colocated in planes parallel to the substrate surface.

We conclude that the THEO part of the SAM of **3** is oriented normal to the Au surface from further analysis of the 1600−800 cm^{-1} region. Comparison of the isotropic and reflectance spectra of **3** (Table 3) reveals that only A_2 bands are observed in the 1600−800 cm^{-1} region. In the isotropic spectrum both the A_2 and E_1 bands of FCC−PEO are observed. In the reflectance spectrum, the E_1 modes, which have transition moments perpendicular to the THEO chain axis, are not observed. The RAIRS spectra were obtained using *p*-polarized light, which has its electric vector normal to the substrate surface. As a result, only vibrational modes that have a component of their transition moments normal to the substrate surface will be observed. If E_1 transitions are occurring parallel to the surface, which they would be if the THEO chain

(43) Takahashi, Y.; Tadokoro, H. *Macromolecules* **1973**, *23*, 672.
(44) Kobayashi, M.; Sakashita, M. *J. Chem. Phys.* **1992**, *96*, 748.
(45) The unit cell has the parameters $a = 8.05$ Å, $b = 13.04$ Å, c(fiber axis) = 19.48 Å, and $\beta = 125.4°$ and the space group $P2_1/a$-C_{2h}. The five symmetry species are approximations due to the distortion of the PEO structure from the point group D_7.[43] Only the normal modes of the A_2 and E_1 series are infrared active.[44]

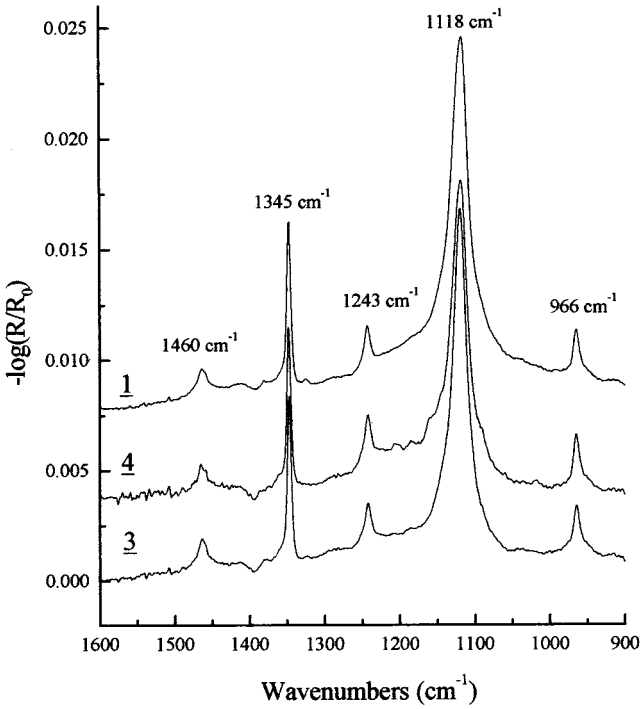

Figure 4. RAIRS spectra of $C_{10}H_{21}(OCH_2CH_2)_6SH$ (**1**), $C_{18}H_{37}(OCH_2CH_2)_6SH$ (**3**), and $C_{18}D_{37}(OCH_2CH_2)_6SH$ (**4**) SAMs from 1600 to 900 cm^{-1}.

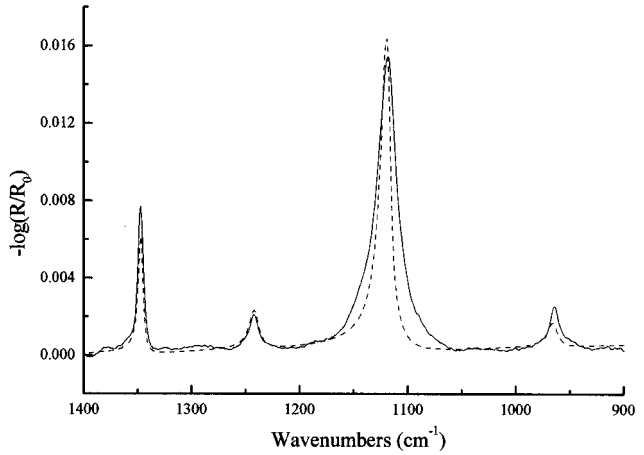

Figure 5. RAIRS spectra of $C_{18}H_{37}(OCH_2CH_2)_6SH$ (**3**) SAM from 400 to 900 cm^{-1} (—) and simulated IR spectra of a SAM of the FCC polymorphic form (- - -) calculated using isotropic spectral data of $C_{18}H_{37}(OCH_2CH_2)_6SH$ (**3**) in KBr.

axes were perpendicular to the surface, they would not be observed. We conclude therefore that the THEO chain is oriented normal to the Au substrate. These conclusions are supported by simulation of the 1400−900 cm^{-1} region, as shown in Figure 5. An excellent correlation between the simulated and observed spectra for **3** was obtained. The correlation of the experimental and simulated spectra did not change with changes in the twist and azimuthal angles, indicating that the THEO segment of the SAM is uniaxial with the helix oriented normal to the surface (0° ± 2°). The slight differences observed between simulation and experiment in Figure 6 are likely due to differences between the optical constants of **3** in the bulk and the monolayer.

The lack of tilt in the hydrophilic segment of the SAM of **3** is undoubtedly due to the width of the helix. We estimate the diameter of the 7/2 helix to be 5.0 ± 0.3 Å based on molecular modeling and estimates from the X-ray

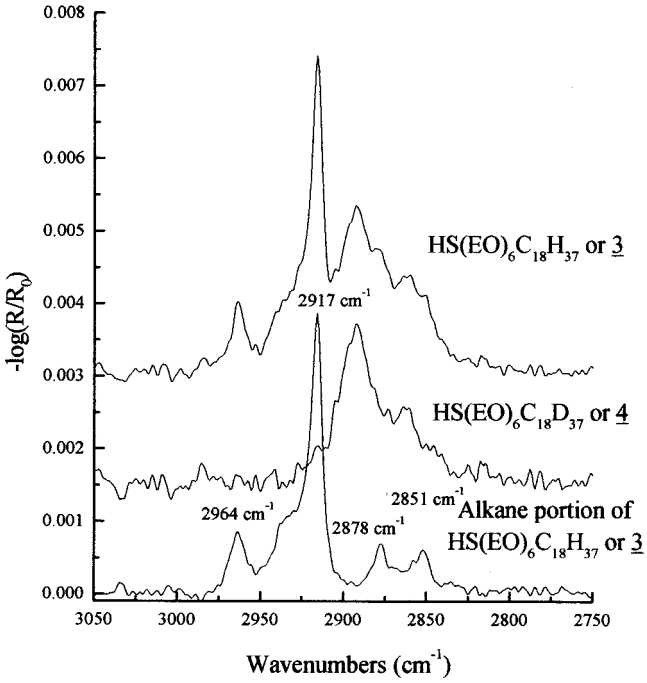

Figure 6. RAIRS spectra of $C_{18}H_{37}(OCH_2CH_2)_6SH$ (**3**) and $C_{18}D_{37}(OCH_2CH_2)_6SH$ (**4**) SAMs from 3050 to 2750 cm^{-1} and their difference spectrum (bottom).

unit cell dimensions of PEO.[43] The cross sectional area of 21.38 Å²/OEO helical segment was obtained from the X-ray unit cell dimensions of PEO. Assuming that our polycrystalline Au surfaces consist predominantly of (1 1 1) facets, the cross sectional area of the THEO segment perfectly matches an idealized packing density (21.4 Å²/thiolate)[32] of a $(\sqrt{3} \times \sqrt{3})R30°$ adlayer on Au with S···S ≅ 5 Å.

Analysis of the 3050−2750 cm^{-1} region of the RAIRS spectrum of **3** reveals the structure of the hydrophobic segment. The 3050−2750 cm^{-1} region of **3** and **4**, as well as the difference spectrum of the two, are shown in Figure 6. The spectrum of the octadecyl-d_{37} compound, **4**, reveals the THEO C−H stretching components, which overlap with C−H stretching vibrational bands of the octadecyl chain. The RAIRS difference spectrum (bottom of Figure 6) obtained from the subtraction of the spectrum of **4** from the spectrum of **3** reveals the positions and relative intensities of the C−H stretching absorption bands of the octadecyl chain. Previous analysis of these absorption bands has laid the groundwork for the determination of the order and the tilt of SAMs on metal substrates.[24,25,32,46,47] The correlation between the position of the asymmetric and symmetric methylene C−H stretching bands, d^- and d^+ respectively, with the degree of order of the SAM is now well established. In the difference spectrum in Figure 6 these absorption bands appear at 2917 and 2851 cm^{-1}, respectively, virtually identical with those obtained for *n*-octadecanethiol (2917 and 2850 cm^{-1}, respectively[24]). Thus the octadecyl chain of **3** is well-organized in a (nearly) fully extended trans conformation.

Assessment of the orientation of the alkyl chain was obtained by simulation of the C−H stretching region of the RAIRS difference spectrum, and the best fit simulated spectrum (dashed line) is shown in Figure 7. The simulated results are consistent with a uniaxial sample with

(46) Nuzzo, R. G.; Dubois, L. H.; Allara, D. L. *J. Am. Chem. Soc.* **1990**, *112*, 558.
(47) Laibinis, P. E.; Whitesides, G. M.; Allara, D. L.; Tao, Y.-T.; Parikh, A. N.; Nuzzo, R. G. *J. Am. Chem. Soc.* **1991**, *113*, 7152.

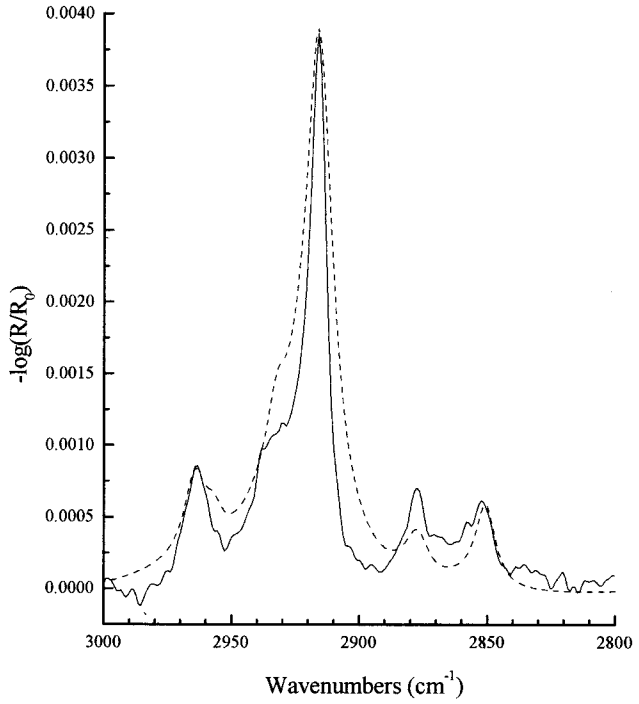

Figure 7. RAIRS spectrum of $C_{18}H_{37}(OCH_2CH_2)_6SH$ (**3**) SAM (—) and simulated spectrum of **3** SAM (- - -) from 3000 to 2800 cm^{-1}.

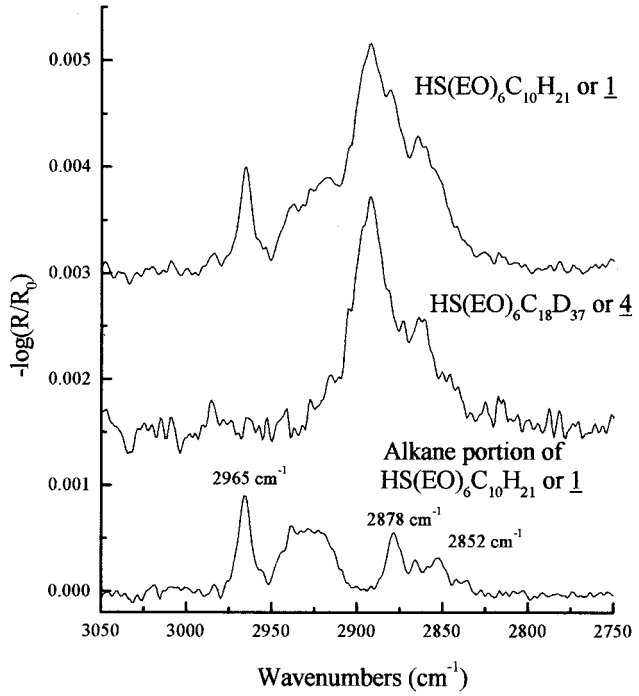

Figure 8. RAIRS spectrum of $C_{10}H_{21}(OCH_2CH_2)_6SH$ (**1**) and $C_{18}D_{37}(OCH_2CH_2)_6SH$ (**4**) SAMs from 3050 to 2750 cm^{-1} and their difference spectrum (bottom).

a tilt angle of 32° ± 2° to the normal of the substrate, similar that found for other long chain (>C_{11}) *n*-alkanethiols, and a twist angle of −30° ± 2°.

The structure of **1** is similar to that of **3**. As indicated earlier, the RAIRS spectrum of **1** and **3** differ only in the C−H stretching region (see Figures 3 and 8). The identical spectral features in the 1600−900 cm^{-1} range indicate that **1** and **3** have identical structures in the THEO portion of their monolayers. The C−H stretching bands of **1** are revealed in the difference spectrum, obtained by subtraction of the RAIRS spectrum of **4** from the RAIRS spectrum of **1**, as shown in Figure 8. This spectrum is similar to that obtained previously for *n*-decanethiol on Au,[20] indicating a comparable degree of order, i.e., a largely extended trans conformation. However, the slight shift in the methylene d^- and d^+ bands (Figure 8) indicates that the alkane portion of **1** is slightly less ordered relative to **3**.

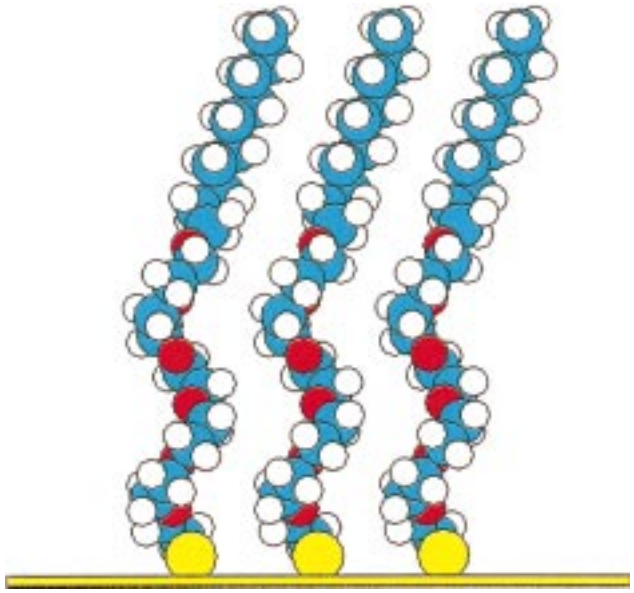

Figure 9. Schematic illustration of the SAM structure of $C_{10}H_{21}(OCH_2CH_2)_6SH$ (**1**) on Au. Sphere color code = type of atom: blue = carbon; red = oxygen; yellow = sulfur; white = hydrogen.

As a result of our IR analysis, we conclude the structure of the SAMs of **1**−**4** to be that indicated in Figure 9 with increased order observed for longer alkyl groups. A somewhat analogous but inverted structure has recently been postulated for the SAM of **5** based on IR data.[48] This report also concludes that the hexa(ethylene oxide) segment has a helical structure oriented normal to the substrate. We obtained a RAIRS spectrum of **5** (data not shown) similar to the "average" spectrum previously reported.[48] All the recently reported spectra of **5**[48] are significantly different in the 1600−900 cm^{-1} region[49] from that found for **1**−**4**. On the basis of the data we present here, which indicate the THEO segment of the SAMs of **1**−**4** to be in a well-ordered 7/2 helix, we infer that the hexa(ethylene oxide) segment of the SAMs of **5** are more amorphous than the THEO segment of **1**−**4**.

Our data show that the SAMs of **1**−**4** are more ordered than our preliminary expectations. This surprising degree of "inflexibility" may leave little space for extramembranous protein segments and water and thus may not be optimal for protein incorporation. However, useful supported HBM constructs will, in all likelihood, not be composed of homogeneous SAMs. Recent studies[1,2,4,5] have employed the OEO motif as "pillars" in mixed SAMs. The relative utility of this approach and monolayer transfer of hydrated **1**−**4** from a Langmuir−Blodgett trough are

(48) Harder, P.; Grunze, M.; Dahint, R.; Whitesides, G. M.; Laibinis, P. E. *J. Phys. Chem.* **1998**, *102*, 426.

(49) The dominant feature in the 1600−900 cm^{-1} region of the spectra of **5** is a series of broad absorption bands at 1114, 1130, and 1145 cm^{-1}. These absorption bands do not correlate with either FCC− or ECC−PEO, which display their most prominent peaks at 1118 and 1099 cm^{-1}, respectively. However, the relatively sharp peaks at 1348, 1244, and 964 cm^{-1}, in the "highly crystalline" spectrum are close to the $A_2(4)$, $A_2(5)$, and $A_2(7)$ bands of FCC−PEO (1345, 1243, and 966 cm^{-1}, respectively[44]).

part of our ongoing investigations and will be the subject of future reports.

Conclusions

Alkylated 1-thiahexa(ethylene oxide) compounds are amphiphiles that form highly ordered, densely packed monolayers on Au, as shown in Figure 9. Analysis of the 1600−900 cm^{-1} region of the RAIRS spectra of the SAMs clearly indicates that the THEO portions of **1**−**4** adopt a lamellar-type crystal morphology in an ordered 7/2 helical structure oriented normal to the substrate. On the basis of the published crystallographic data,[43] we calculate a thickness of 16.6 Å for the THEO segment in the 7/2 conformation. In contrast, we estimate a thickness for the THEO segment in an all-trans extended conformation of 20.5 Å (Hyperchem). Both the RAIRS and inferences from our ellipsometric data suggest a thickness of ∼16 Å for the THEO portion of the SAMs of **1**−**4**, consistent with the helical conformation. Analysis of the CH stretching region (3050−2750 cm^{-1}) for **3** shows that the alkyl tail is essentially in a nearly fully extended trans conformation tilted at 32 ± 2° to the normal. For the shorter chain compound **1**, the alkyl chain is less ordered and the angle of the tilt is less certain. With identical structures in the THEO segment, monolayers of hydrocarbon chains that are fully trans extended and tilted at ∼30° should exhibit a thickness increase of ∼1.2 Å/CH_2,[21] consistent with the 10 Å difference in the ellipsometry for the C_{10} and C_{18} compounds.

Acknowledgment. The authors would like to express appreciation to Adrian Roitberg for assistance in some of the modeling of the THEO segment of these compounds.

LA9806451